

# Bayesian Analysis of Combustion Kinetic Models for Ammonia-Hydrogen Fuel Blends Using Artificial Neural Networks

Guanyu Wang<sup>1\*</sup>, Fan Wang<sup>2</sup>, Michael Jones<sup>3</sup> and Solmaz Nadiri<sup>1</sup>

<sup>1</sup>Department of Physical Chemistry, Physikalisch-Technische Bundesanstalt, 38116 Braunschweig, Germany

<sup>2</sup>Faculty of Mathematics, Otto-von-Guericke-University Magdeburg, Universitätsplatz 2, 39106 Magdeburg, Germany

<sup>3</sup>Queen's University Kingston, 99 University Avenue, Kingston, Ontario, K7L 3N6, Canada

**Abstract.** Uncertainty quantification (UQ) plays a crucial role in predictive modeling in combustion chemistry, as it improves the accuracy of predictions and the reliability. To accurately predict ignition delay times and nitrogen oxides (NO<sub>x</sub>) emissions of ammonia (NH<sub>3</sub>) and hydrogen (H<sub>2</sub>) fuel blends, minimizing uncertainty in combustion kinetic models is critical. This study introduces a novel approach that integrates Bayesian analysis with Artificial Neural Networks (ANNs) to perform inverse UQ and update combustion kinetic models based on experimentally measured nitric oxide (NO) speciation time history. Traditional Markov Chain Monte Carlo (MCMC) methods are effective, but they are computationally intensive and require large datasets, which limit their practical applicability. ANNs are applied as surrogate models to replace traditional kinetic modeling, optimizing the combustion kinetic model of NH<sub>3</sub>/H<sub>2</sub> fuel blends. By integrating Bayesian analysis with ANNs, the computational cost was significantly reduced compared to conventional MCMC methods, while maintaining high accuracy in uncertainty quantification and parameter optimization. This approach facilitates efficient exploration of parameter space and ensures reliable predictions, making it a valuable tool for complex combustion modeling.

## 1 Introduction

The transition to carbon neutrality requires the adoption of efficient, low-carbon alternative fuels. Ammonia (NH<sub>3</sub>), recognized as a promising zero-carbon fuel, offers significant advantages such as ease of storage and transport. However, its application is limited by slow combustion rates and the production of nitrogen oxides (NO<sub>x</sub>) when burned alone. Blending ammonia with hydrogen (H<sub>2</sub>) enhances combustion performance by reducing ignition delay times (IDTs) and NO<sub>x</sub> formation.

Accurate prediction of the combustion process through kinetic modeling is essential for improving the efficiency and reliability of energy systems. To improve these models, Inverse Uncertainty Quantification (UQ) is used to minimize uncertainty in predictions by refining model parameters based on experimental data. The concept of inverse UQ for kinetic models was introduced by Frenklach et al. [1], and methods like data collaboration and solution mapping techniques have been instrumental in refining models such as GRI-Mech 3.0 [2]. The Bayesian method is a probabilistic approach to tackle inverse UQ. By incorporating prior knowledge of system parameters and uncertainties, Bayesian analysis utilizes stochastic sampling to produce posterior distributions for model parameters and predictions. Wang and Sheen [3] explained that Bayesian methods provide probabilistic estimates of rate parameters, which improves predictive reliability by

quantifying uncertainties and enabling more accurate extrapolation beyond the range of experimental data. A key technique in Bayesian analysis is Markov Chain Monte Carlo (MCMC), which iteratively generates correlated samples from posterior distributions. Although MCMC is widely employed, its computational demands make it challenging to apply to high-dimensional combustion models, often limiting its practical use to simpler combustion systems or smaller reaction sets.

Bayesian methods become increasingly challenging for complex systems, such as ammonia-hydrogen fuel blends. To improve computational efficiency, recent studies have integrated Artificial Neural Networks (ANNs) with MCMC, using ANNs as surrogate models to approximate combustion behavior. By capturing nonlinear relationships, ANNs enable faster and more scalable optimization, making Bayesian analysis feasible for high-dimensional systems. Wang et al. [4] introduced an ANN-assisted MCMC approach that improves the efficiency of Bayesian inverse UQ in combustion kinetics. They utilized ANNs as surrogate models, significantly reducing computational costs while maintaining accuracy in estimating the posterior distributions of kinetic parameters. This approach is particularly beneficial for complex combustion systems with restricted computational resources.

This study integrates Bayesian analysis with ANN-based surrogate models to perform inverse uncertainty quantification for ammonia-hydrogen fuel blend

\* Corresponding author: [guanyu.wang@ptb.de](mailto:guanyu.wang@ptb.de)

combustion. By utilizing time-resolved NO concentration data [5], this approach optimizes pre-exponential factors (A-factors) in the Arrhenius equations, which are crucial for accurately predicting IDTs and NO emissions. By using surrogate models, we were able to reduce the computational effort compared to traditional MCMC methods, which makes Bayesian analysis more efficient and accessible for complex kinetic models. This approach provides a scalable framework that enhances the accuracy of combustion simulations, serving as a valuable tool for optimizing fuel blends and improving the sustainability of energy systems.

## 2 Methodology

Unlike the Frequentist approach, where parameters are assumed to be fixed but unknown, Bayesian methods treat parameters as probability distributions that can be updated with experimental data. In this work, the Bayesian approach is implemented to calibrate the simulation results from the knowledge of experiment data.

### 2.1 The Bayesian inference

Apart from the Frequentist approach, the true distribution of the is assumed unknown thus the parameters of the distribution are undetermined as well. The Bayesian Approach provides a way to inference the distribution as well as its parameters from the data sampled from the true distribution which is shown in the Equation (1),

$$p_{\text{post}}(\boldsymbol{\theta}|\mathbf{d}) = \frac{p_{\text{prior}}(\boldsymbol{\theta})p(\boldsymbol{\theta};\mathbf{d})}{\int p_{\text{prior}}(\boldsymbol{\theta})p(\boldsymbol{\theta};\mathbf{d})d\boldsymbol{\theta}} \quad (1)$$

where  $p_{\text{post}}(\boldsymbol{\theta}|\mathbf{d})$  is the posterior distribution which is the inferred distribution of the parameters  $\boldsymbol{\theta}$ , and  $\mathbf{d}$  is the given measurement data from the experiments. The Bayesian formula gives the possibility to calibrate inferred posterior distribution of the kinetic parameters according to the measurement of the experiments. The numerator of the right-hand side of the Equation (1) is multiplication between prior distribution of parameters  $\boldsymbol{\theta}$  and likelihood function of collected experiment data  $\mathbf{d}$ . The prior distribution reflects the prior knowledge of  $\boldsymbol{\theta}$  and the posterior influences the posterior significantly.

Meanwhile, the likelihood function models the uncertainty of the measurement. With the injection of measurement form experiment, the posterior is updated by leveraging the prior belief and likelihood of the measurements. While the integral term in the denominator, is known as the normalising or constant term, which is intractable. Therefore, we don't compute it explicitly. Hence the Equation (1) can be simplified as Equation (2) as follows

$$p_{\text{post}}(\boldsymbol{\theta}|\mathbf{d}) \propto p_{\text{prior}}(\boldsymbol{\theta})p(\boldsymbol{\theta};\mathbf{d}) \quad (2)$$

The prior distribution of  $\boldsymbol{\theta}$  can be determined by the prior knowledge of  $\boldsymbol{\theta}$ , a common choice is uniform

distribution or Gaussian distribution. We use uniform distribution as the parameters are uniformly sampled from the given sample domain. Besides the choice of prior, the choice of likelihood affects the quality of the posterior significantly as well. We use the multiplicative error model as suggested from [4]. And the likelihood is formulated as follows in Equation (3) and Equation (4):

$$p(\mathbf{x};\mathbf{d}) = C \cdot \exp\left[-\frac{1}{2}\sum_{i=1}^N\left(\frac{\ln x_i - \ln d_i}{\sigma_i}\right)^2\right] \quad (3)$$

$$C = \frac{1}{\prod_{i=1}^N\sqrt{2\pi\sigma_i^2}} \quad (4)$$

where N represents the total number of sample pairs of simulated results  $\mathbf{x}$  and the collected experiment measurements  $\mathbf{d}$ . In which  $x_i$  and  $d_i$  are the sample pair for simulation and experiment respectively with identical parameter input. Variance  $\sigma_i^2$  characterizes the uncertainty of the experimental measurement. Since the posterior distribution is not a known distribution, there is so analytic solution of it, it will be practically obtained by running MCMC simulation.

### 2.2 Markov Chain Monte Carlo

Bayesian inference is useful to infer the distribution of the parameters from the know information of the measurements, it combines prior knowledge with new data to compute a posterior distribution using Bayes' theorem. However, computing the posterior analytically is often infeasible in complex models. MCMC methods address this by providing a way to sample from the posterior distribution. MCMC uses a Markov chain to explore the sample space, generating samples that approximate the target distribution. This sampling approach makes MCMC an useful tool for solving high-dimensional problems in Bayesian analysis, particularly when direct integration is impossible. There are many ways to realize MCMC, and we used the Metropolis–Hastings (MH).

MH algorithm is a common method for MCMC for generating samples from a target distribution. It works by constructing a Markov chain with the desired distribution as its stationary distribution. At each step, a candidate sample is proposed from a proposal distribution, and then accepted or rejected based on a probability determined by the ratio of the target distribution to the proposal distribution. If accepted, the candidate becomes the new state; if otherwise, the chain stays at the current state. MH is flexible and can be applied to distributions with intractable normalizing constants.

### 2.3 Surrogate models

The ANN used in this work is a Multilayer Perceptron (MLP), employed as a surrogate model to approximate complex, high-dimensional non-linear simulations. It features GELU activation functions, AdamW optimizer for adaptive learning rates, and a batch size of 256 for efficient training. Regularization techniques, including

dropout and batch normalization, are applied to prevent overfitting and ensure robust performance, making the model both computationally efficient and accurate in capturing complex relationships. Detailed settings are shown in Section. 4.2.

### 3 Kinetic modelling

The simulation of time-resolved NO concentration in the shock tube was conducted using an in-house Cantera code (version 3.0.0) [6] with a constant volume, 0-D homogeneous adiabatic, ideal gas reactor model. The kinetic model of ammonia hydrogen blend oxidation developed by Solmaz et al. [7] is employed for this study. The model contains 87 species and 460 reactions. To enhance the computational efficiency of the MCMC sampling process, the model was reduced to 50 reactions, focusing on the most influential reactions for NH<sub>3</sub>/H<sub>2</sub> blend oxidation. This reduction significantly improved the efficiency of the optimization procedure while preserving the accuracy necessary for reliable predictions of ignition delay and emissions. The uncertainty factor (UF) for a reaction rate is defined as:

$$F = \frac{k_0}{k_{min}} = \frac{k_{max}}{k_0} \quad (5)$$

where  $k_0$  is the nominal value of the rate coefficient,  $k_{max}$  and  $k_{min}$  represent the upper and lower bounds of the rate coefficient, respectively. Each rate coefficient  $k_i$  is assumed to follow a prior log-uniform distribution within the uncertainty range ( $k_{min}$ ,  $k_{max}$ ). The uncertainty factors for the rate coefficients were derived from literature compilations [8, 9]. A brute-force sensitivity analysis was performed for both IDT and the maximum NO concentration across all mixtures at three different temperatures: 1600 K, 1800 K, and 2000 K. In this approach, the rate coefficients of all reactions in the mechanism are individually doubled in each cycle, with the solver initialized to the reactor's starting conditions ( $T_5$ ,  $P_5$ ). The reactions identified as the top ten most sensitive for both IDT and NO maximum concentration are then compiled, resulting in a total of 29 reactions. These reactions were selected for further analysis in the MCMC study.

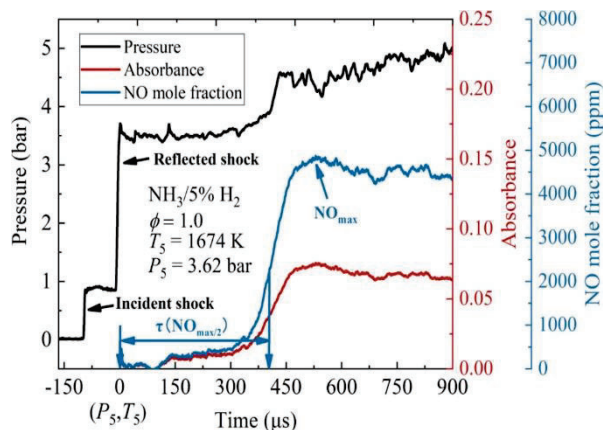


**Figure 1.** Measured pressure, absorbance, NO profile, and the definition of two characteristic parameters for the case of NH<sub>3</sub>/5%H<sub>2</sub> mixture [5].

The experimental data used in this work was obtained from Zhu et al. [5] [10] includes pure NH<sub>3</sub> and ammonia-hydrogen blends with hydrogen concentrations of up to 20%. Fig. 1 illustrates a typical measured NO time history for NH<sub>3</sub>/H<sub>2</sub> blend in a shock tube. Two characteristic parameters were extracted from the NO time histories for more detailed quantitative analysis: NO<sub>max</sub>, which represents the maximum NO mole fraction, and  $\tau(\text{NO}_{\text{max}/2})$ , the time from time zero ( $P_5$ ,  $T_5$ ) to the time corresponding to the position of half of the NO<sub>max</sub>. These parameters capture the amplitude and phase of the NO profiles, respectively. And they represent the experimental data used in this work.

## 4 Results and discussion

### 4.1 Cantera-based MCMC

Sensitivity analyses (SAs) were performed to identify the most influential reactions in the kinetic model for both IDT and maximum NO mole fraction (NO<sub>max</sub>). Fig. 2 illustrates an example of sensitivity analysis for IDT at a temperature of 2000 K and a pressure of 3.0 bar. Following the analysis, 29 key reactions were selected as the most important for both IDT and NO<sub>max</sub>, based on their impact on the model predictions.

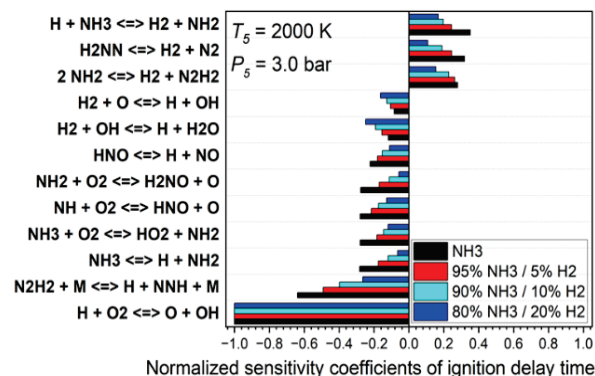


**Figure 2.** Sensitivity analysis of the IDT for all experimental conditions at  $T_5 = 2000\text{K}$ ,  $P_5 = 3$  bar

Following the sensitivity analysis results, the traditional MCMC method with the Metropolis-Hastings algorithm was used to sample reaction coefficients for the kinetic model, with the goal of minimizing discrepancies between model predictions and experimental data. This involved conducting a series of simulations to sample reaction rate coefficients (log A factors) and iteratively minimize the discrepancy between the model predicted values and experimental measurements. The MH algorithm proposed new values for the reaction rate coefficients, which were accepted or rejected based on the likelihood of improving the model fit to the experimental data.

The optimization process involved conducting 100,000 MCMC iterations, with convergence generally achieved after approximately 30,000 steps. In each iteration, the model was evaluated by computing the discrepancy between the simulated and experimental values, such as IDT and maximum NO mole fraction. These discrepancies were used to calculate the

likelihood of each proposed set of reaction rate coefficients, guiding the MH algorithm to accept or reject the proposed solutions based on their relative likelihood. The mechanism that minimized the discrepancies was identified by evaluating the posterior distribution of the model parameters. This evaluation provided the most probable values for the reaction rate coefficients. As a result, the optimization process produced a refined set of log A factors, which significantly enhanced the model's predictions for both IDT and the maximum mole fraction of NO.

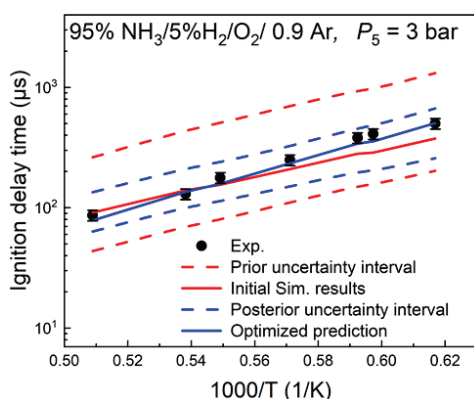


**Figure 3.** Comparison of the prior and posterior distributions of ignition delay time for 95% NH<sub>3</sub> / 5% H<sub>2</sub> fuel blends

Fig 3 shows the comparison of the prior and posterior distributions of IDT for 95% NH<sub>3</sub> / 5% H<sub>2</sub> fuel blends based on MCMC analysis. The measured data with an error bar  $\pm 10\%$ . The prior uncertainty interval was derived using Latin Hypercube Sampling for the rate coefficients within their uncertainty bounds, coupled with Cantera simulations. The posterior uncertainty interval was calculated from the output of the Cantera-based MCMC process. Notably, the posterior uncertainty interval is narrower than the prior, indicating a reduction in uncertainty. The optimized predictions (blue line) represent the best model generated during the MCMC process, and these predictions show a significantly improved match with the experimental data across the entire temperature range.

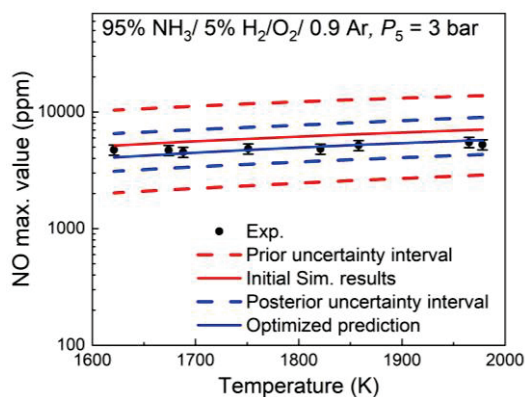


**Figure 4.** Comparison of the prior and posterior distributions of NO maximum value for 95% NH<sub>3</sub> / 5% H<sub>2</sub> fuel blends

Fig. 4 shows a comprehensive comparison of the prior and posterior distributions of the maximum NO mole fraction for 95% NH<sub>3</sub> / 5% H<sub>2</sub> fuel blends based on

MCMC analysis. The method for deriving the prior and posterior uncertainty intervals was the same as for the IDT. The experimental data, shown with error bars representing a  $\pm 10\%$  uncertainty, is compared with the optimized predictions (blue line). The optimized mechanism shows significantly better results, with all the data points located within the uncertainty bounds.

Fig. 5 shows two examples of the NO time history for the 95% NH<sub>3</sub> / 5% H<sub>2</sub> fuel blends under different conditions. The left panel corresponds to  $T = 1859$  K and  $P = 3.26$  bar, while the right panel represents  $T = 1621$  K and  $P = 3.64$  bar. The NO peak value ( $\text{NO}_{\text{max}}$ ) and the time to reach half of the NO peak ( $\tau(\text{NO}_{\text{max}/2})$ ) are key parameters that capture the amplitude and phase of the NO profiles, respectively.  $\text{NO}_{\text{max}}$  and  $\tau(\text{NO}_{\text{max}/2})$  were used in the MCMC process as discrepancy measures and for likelihood calculations. The predicted values for these parameters were optimized during the MCMC process by comparing the simulated data with experimental measurements. The optimized model (blue) provides a significantly improved match to the experimental data (black) for both NO peak and phase, compared with the original model (red).

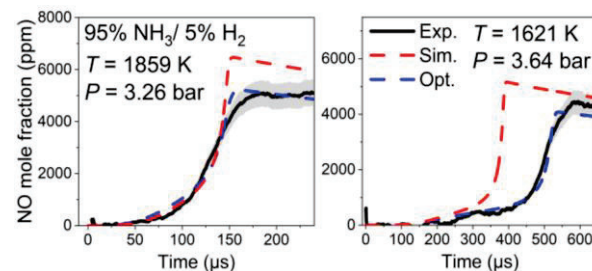


**Figure 5.** Comparison of measured NO mole fraction with original kinetic model and optimized model for 95% NH<sub>3</sub> / 5% H<sub>2</sub> fuel blends

## 4.2 ANN-based MCMC

### 4.2.1 ANN training result

The ANN framework is based on an MLP architecture implemented using the PyTorch framework. The ANN has 35 input features, which include gas compositions, temperature, pressure, and reaction rates, and two output targets: the log of the IDT and the peak NO value. The model architecture consists of 6 hidden layers with progressively fewer nodes. The training dataset, which consists of 310,000 data points, is generated from Cantera simulations. The dataset is split into 70% for training, 15% for validation, and 15% for testing. Data preprocessing involves scaling both the input features and target variables using StandardScaler to normalize the data and improve model convergence. The model is trained to minimize the mean relative error (MRE), and the learning rate is dynamically adjusted during training. The model's performance is evaluated using two metrics:  $R^2$  and MRE. Predictions are compared against experimental data for NO emissions and IDT. Regularization techniques like dropout and batch normalization are applied to prevent overfitting and enhance generalization.

Fig.6 illustrates the training progress of the ANN model, with the MRE and R<sup>2</sup> values plotted against the number of epochs, based on the validation set. As shown, the MRE decreases significantly during the initial training epochs, dropping from approximately 0.02 to 0.006 within the first 50 epochs. The R<sup>2</sup> value increases steadily and reaches 0.999 towards the end of the training, indicating a near-perfect correlation between the predicted and actual values. These results demonstrate that the model effectively learned the underlying relationships in the data, providing highly accurate predictions with minimal uncertainty.

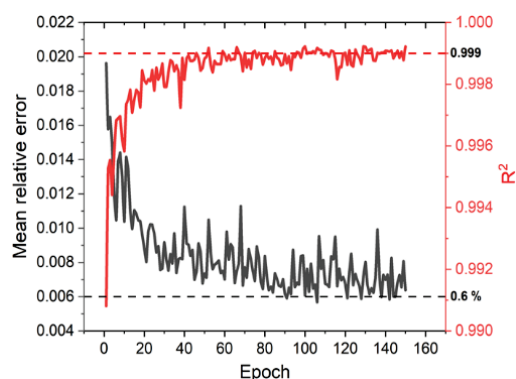


**Figure 6.** ANN Training Progress: MRE and R<sup>2</sup> vs. Epochs

#### 4.2.2 Comparison of MCMC and ANN MCMC

This section compared the performance of traditional MCMC with the ANN-MCMC. Integrating ANNs with MCMC provides a robust framework for optimizing kinetic models and enhances optimization efficiency.

A time comparison between the ANN-MCMC approach with 100,000 steps and the traditional MCMC process is shown in Table 1. The results indicate that the ANN-MCMC approach significantly reduces overall computation time, with a total of 2203 seconds, compared to 170,905 seconds for the traditional Cantera-MCMC method. The key difference is observed in the model evaluation step, where Cantera-MCMC takes 170522 seconds, while the ANN-MCMC method requires only 326 seconds. However, the ANN training process adds 1504 seconds. The overall efficiency gain is considerable, as the combination of ANN and MCMC results in more than a 70-fold reduction in computation time. This demonstrates the effectiveness of the ANN-based optimization in accelerating the modeling process without sacrificing accuracy.

**Table 1:** Comparison of Computational Time: Cantera + MCMC vs. ANN + MCMC

	Cantera-MCMC	ANN-MCMC
Model evaluation	170522 s	326 s
Training of ANN	-	1504 s
MCMC process	331 s	324 s
Save the results	52 s	49 s
Total	170905 s	2203 s

To get a more detailed and accurate exploration of the parameter space, we expanded the number of steps to 1 million in the ANN-MCMC approach to further enhance the optimization process. Traditional 100,000 steps MCMC processes may fail to fully capture the complexity of non-linear systems, potentially missing important regions of the parameter space. Increasing the number of steps can achieve a much finer resolution in the posterior distributions, leading to a more reliable and accurate model. This extensive sampling ensures that the posterior distributions are well-converged and accurately reflect the joint distributions of the parameters, thereby improving the overall quality of the model's predictions.

Fig. 7 shows the prior and posterior distributions of the log A factors for two key reactions in the model. The prior distributions reflect the initial uncertainty in the reaction rate coefficients. These prior distributions capture a broad range of possible values before optimization. The posterior distributions (blue curves) are obtained from the ANN-MCMC optimization process with 1 million steps. The left plot corresponds to the reaction  $H + O_2 \rightleftharpoons O + OH$ , where the prior distribution of the log A factor is centered around 14.98. After the MCMC process, the posterior distribution shifts slightly to 15.045, showing a small increase in the rate constant. The right plot shows the reaction  $NH_3 + H \rightleftharpoons NH_2 + H_2$ . Similarly, the log A factor shifts from the prior center 5.81 to the posterior center 5.76 after the MCMC process, reflecting a slight decrease in the rate constant for this reaction. The figure shows that the posterior distributions are narrower than the priors, indicating a reduction in uncertainty after the optimization. The optimized predictions provide more precise values for the rate coefficients, leading to a more accurate model.

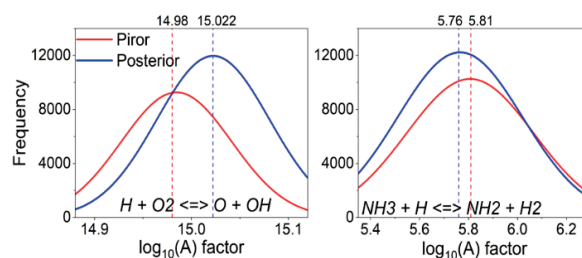


**Figure 7.** Comparison of Prior and Posterior Distributions for Reaction Rate Constants

Fig. 8 illustrates the joint distribution of the two reaction rate constants,  $H + O_2 \rightleftharpoons O + OH$  and  $NH_3 + H \rightleftharpoons NH_2 + H_2$ , as shown in the contour plot. The plot shows the density of the log(A) factors, with darker shades indicating higher density and lighter shades representing lower density. The contours reveal the correlation between the two rate constants, illustrating regions of high probability where both rate constants are most likely to occur. The distribution indicates a strong relationship between the rate constants of the two reactions, with the densest regions concentrated around a specific set of values, indicating the most probable optimized rate constants. This joint distribution provides insights into the uncertainty and interactions between the rate constants, identifying the regions of parameter

space with the greatest likelihood of accurate predictions.

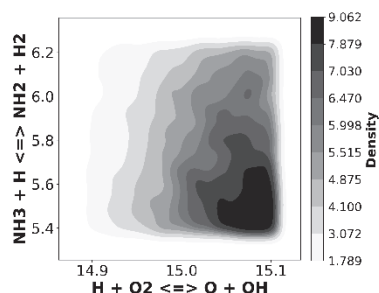


**Figure 8.** 2D Joint Distribution of Reactants and Products:  $\text{H} + \text{O}_2 \rightleftharpoons \text{O} + \text{OH}$  and  $\text{NH}_3 + \text{H} \rightleftharpoons \text{NH}_2 + \text{H}_2$

## 5 Conclusion

This study presents a practical approach for performing inverse uncertainty analysis on combustion kinetic models of ammonia-hydrogen fuel blends by combining Bayesian analysis with ANNs. The analysis focused on optimizing the pre-exponential factors (A-factors) in the Arrhenius equation, targeting 29 key critical parameters to accurately predict the combustion kinetics of  $\text{NH}_3/\text{H}_2$  fuel blends.

By using ANNs as surrogate models, the computational cost was significantly reduced compared with traditional MCMC methods while still maintaining high accuracy in uncertainty quantification and parameter optimization. This approach provides an effective solution for dealing with high-dimensional systems. The narrower posterior distribution shows that the uncertainty has been reduced, leading to better alignment between the model's predictions and the experimental data. Additionally, the best-performing model is obtained during the MCMC process, ensuring that the optimized model provides reliable and accurate predictions for IDT and NO time history.

This work demonstrates how ANN-assisted Bayesian optimization can improve both the accuracy and efficiency of combustion modeling. By significantly reducing computational costs, this method is particularly useful for dealing with complex fuel blends or larger molecules that require more detailed kinetic models. The results presented here contribute to the broader goal of carbon neutrality, offering a robust tool for predictive modeling in fuel combustion research.

Guanyu Wang acknowledges the funding by the Deutsche Forschungsgemeinschaft (DFG, German Research Foundation) - 390881007, EXC 2163 Sustainable and Energy Efficient Aviation. Fan Wang acknowledges funding by the Deutsche Forschungsgemeinschaft (DFG, German Research Foundation) - 314838170, GRK 2297 MathCoRe.

## References

1. M. Frenklach, H. Wang, and M.J. Rabinowitz, Optimization and analysis of large chemical kinetic mechanisms using the solution mapping method—combustion of methane. *Prog. Energy Combust. Sci.* **18**(1), 47-73 (1992) [https://doi.org/10.1016/0360-1285\(92\)90032-V](https://doi.org/10.1016/0360-1285(92)90032-V).

2. G.P. Smith, D.M. Golden, M. Frenklach, N.W. Moriarty, B. Eiteneer, M. Goldenberg, C.T. Bowman, R.K. Hanson, S. Song, W.C. Gardiner, V.V. Lissianski, and Z. Qin. Available from: <http://www.me.berkeley.edu/gri-mech>.
3. H. Wang and D.A. Sheen, Combustion kinetic model uncertainty quantification, propagation and minimization. *Prog. Energy Combust. Sci.* **47**, 1-31 (2015) <https://doi.org/10.1016/j.peccs.2014.10.002>.
4. J. Wang, Z. Zhou, K. Lin, C.K. Law, and B. Yang, Facilitating Bayesian analysis of combustion kinetic models with artificial neural network. *Combust. Flame.* **213**, 87-97 (2020) <https://doi.org/10.1016/j.combustflame.2019.11.035>.
5. D. Zhu, L. Ruwe, S. Schmitt, B. Shu, K. Kohse-Höinghaus, and A. Lucassen, Interactions in Ammonia and Hydrogen Oxidation Examined in a Flow Reactor and a Shock Tube. *J. Phys. Chem. A.* **127**(10), 2351-2366 (2023) <https://doi.org/10.1021/acs.jpca.2c07784>.
6. D. G. Goodwin, H. K. Moffat, I. Schoegl, R. L. Speth, and B. W. Weber, Cantera: An Object-oriented Software Toolkit for Chemical Kinetics, Thermodynamics, and Transport Processes. (Version 3.0.0)
7. S. Nadiri, B. Shu, C.F. Goldsmith, and R. Fernandes, Development of comprehensive kinetic models of ammonia/methanol ignition using Reaction Mechanism Generator (RMG). *Combust. Flame.* **251**, 112710 (2023) <https://doi.org/10.1016/j.combustflame.2023.112710>.
8. D.L. Baulch, C.J. Cobos, R.A. Cox, P. Frank, G. Hayman, T. Just, J.A. Kerr, T. Murrells, M.J. Pilling, J. Troe, R.W. Walker, and J. Warnatz, Evaluated Kinetic Data for Combustion Modeling. Supplement I. *J. Phys. Chem. Ref. Data.* **23**(6), 847-848 (1994) <https://doi.org/10.1063/1.555953>.
9. D. Baulch, C.T. Bowman, C.J. Cobos, R.A. Cox, T. Just, J. Kerr, M. Pilling, D. Stocker, J. Troe, and W. Tsang, Evaluated kinetic data for combustion modeling: supplement II. *J. Phys. Chem. Ref. Data.* **34**(3), 757-1397 (2005) <https://doi.org/10.1063/1.1748524>.
10. D. Zhu, Z. Qu, M. Li, S. Agarwal, R. Fernandes, and B. Shu, Investigation on the NO formation of ammonia oxidation in a shock tube applying tunable diode laser absorption spectroscopy. *Combustion and Flame.* **246**, 112389 (2022) <https://doi.org/10.1016/j.combustflame.2022.112389>.